5th International Conference on Biaxial/Multiaxial Fatigue and Fracture
Cracow'97, Poland

S. Y. ZAMRIK* and M. L. RENAULD*

A Biaxial Fatigue Model for Thermomechanical Strain Cycling

*The Pennsylvania State University, University Park, PA 16802, USA

Keywords: Biaxial Fatigue, Thermomechanical, Crack Growth, Triaxiality Factor, Z-parameter, Phase Factors

ABSTRACT: A biaxial thermomechanical fatigue (TMF) model has been developed by extending a biaxial fatigue model for isothermal condition. The proposed model assesses the in-phase and out-of-phase type cycle incorporating the effect of oxidation and creep. The isothermal fatigue model utilizes the concept of triaxiality factor (TF) which accounts for the state of stress effect on material's fracture ductility. The TMF biaxial strain ratios varied from 0 to 3.65 at cyclic temperatures of 399-621 °C (750-1150 °F). All tests were strain controlled using tubular specimens. Heating was by induction and cooling was by natural convection.

Notation

$\Delta\varepsilon^{t}_{eq}$	Mises equivalent strain
$\Delta\varepsilon^{in}$	inelastic strain
$\bar{\varepsilon}_f$	effective ductility
ε_{fo}	tensile ductility
γ	shear strain
λ	biaxial strain ratio
ϕ	phase factor
ϕ^{IP}	in-phase factor
ϕ^{OP}	out-of-phase factor
σ_1	principal stress
σ_2	principal stress
σ_3	principal stress
f	frequency
N_f	cycles to failure
T	temperature
TF	triaxiality factor
Z	Z-parameter

Introduction

Thermomechanical fatigue (TMF) has recently surfaced as a major contributor of industrial component failure. The TMF process is a result of thermal cycling superimposed on mechanical load. If the thermal strain is added to the mechanical strain, then the cycle is known as in-phase (IP); however, if the thermal strain is not additive, then the TMF cycle is out-of-phase (OP). The life of structural components is greatly affected by these two types of cycles. For example, in material such as Inconel 738LC, which is a high strength low ductility material used as gas turbine blades, the fatigue life is considerably reduced when the strain and temperature are out-of-phase with each other, while in material such as 316 stainless steel, a low strength and high ductility material, the in-phase condition is more damaging to fatigue life. Also, the life of the component is affected, in addition to the phasing of the TMF cycle, by the state of stress. Since most components experience a multiaxial/biaxial state of stress, basic life prediction models developed for isothermal conditions were found inadequate to address the effect of TMF.

In searching the literature, one finds a limited amount of published results which address TMF and the state of stress. Yamauchi et al. **[1]** established a variable temperature distribution along a pipe specimen by induction heating the outer surface and cooling the inner surface with water. This testing condition generated equal biaxial stress state under out-of-phase loading. The loss in life was attributed to a reduction in the material's ductility. Castelli et al. **[2]** investigated the TMF deformation of Hastelloy X in torsion at three temperature ranges. The emphasis was not on fatigue life prediction but rather on the applicability of the J_2 yield criterion under TMF. The correlation was good at the highest temperature range, but decreased with decreasing temperature. Meerman et al. [3] published biaxial TMF results on IN-738LC where various combinations of stress and strain parameters were used to correlate all fatigue data resulting in limited success. Bonacuse and Kalluri **[4]** investigated the axial, torsion and axial-torsion TMF response of wrought cobalt base superalloy, Haynes 188, at a temperature range of 316-760 °C (600-1400°F) and shear strain ranges of 0.8 % and 1.4 %. They investigated the applicability of four life prediticton models: the von Mises equivalent strain range, the Modified Multiaxiality

Factor, MF [5], the modified Smith-Watson [6] and the Fatemi-Socie-Karath model [7]. The Mises and the Modified Multiaxiality factor methods provided the best data fit.

Material and Test Procedure

Type 316 stainless steel material, used in this research program, was provided by Oak Ridge National Laboratory in the form of 25.4 mm (1 inch) diameter rod hot rolled at 1180 °C. Tubular fatigue specimens were machined from the rolled bars by a low stress grinding process to the dimensions shown in Figure 1.

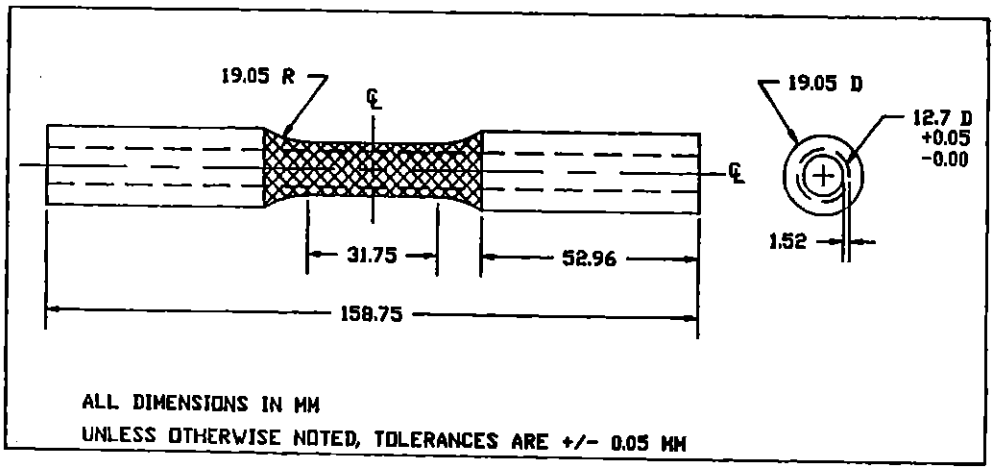

Fig 1. Biaxial TMF test specimen.

Machined specimens were solution annealed at 1065 °C in Argon for 30 minutes. The TMF testing equipment contains three closed-loop control loops, one for temperature and two for mechanical actuator (axial and torsional), as shown schematically in Figure 2. Figure 3 outlines the TMF testing procedure. To monitor axial-torsion strains, an MTS high temperature biaxial extensometer was used. The temperature command procedure for the TMF cycle is shown in Figure 4.

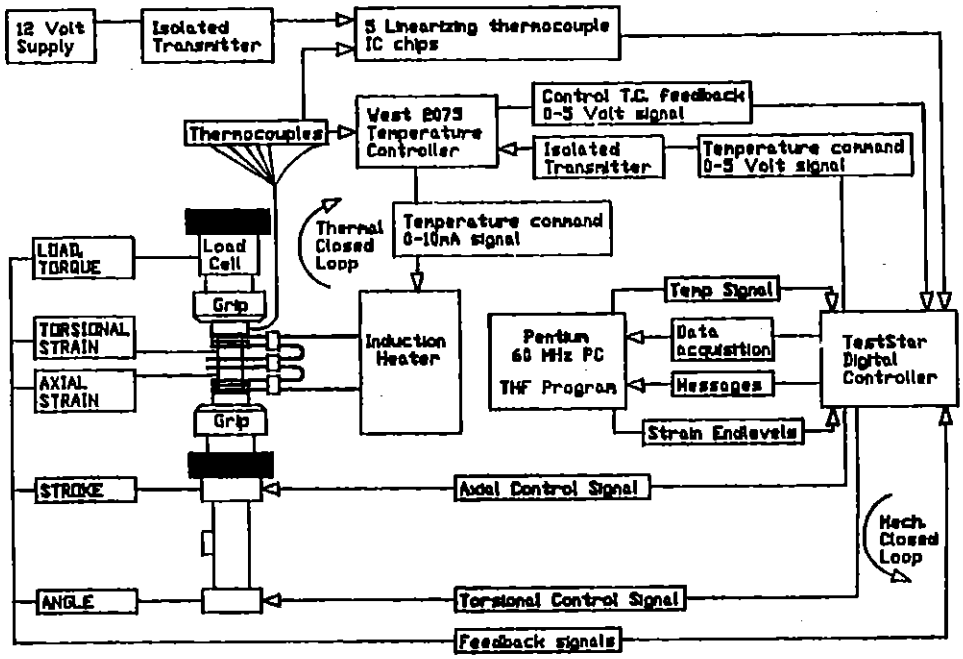

Fig. 2 Schematic of TMF testing system.

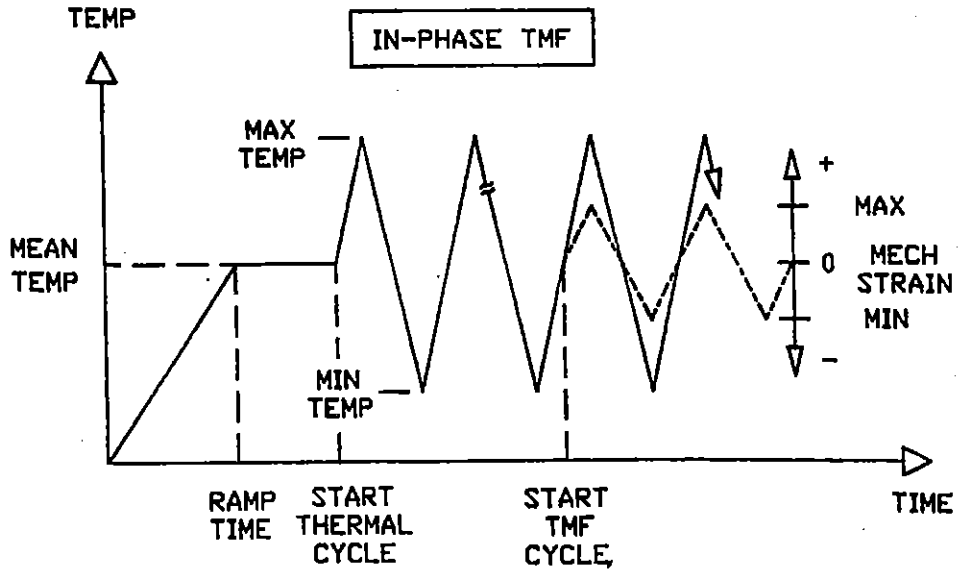

Fig. 3a Relationship between thermal and mechanical strains at start-up of IP TMF test.

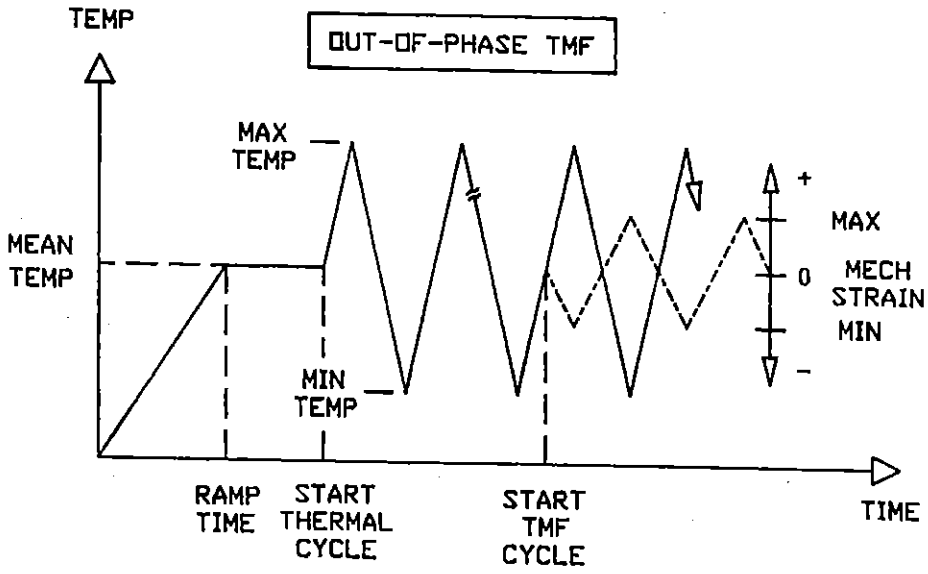

Fig. 3b Relationship between thermal and mechanical strains at start-up of OP TMF test.

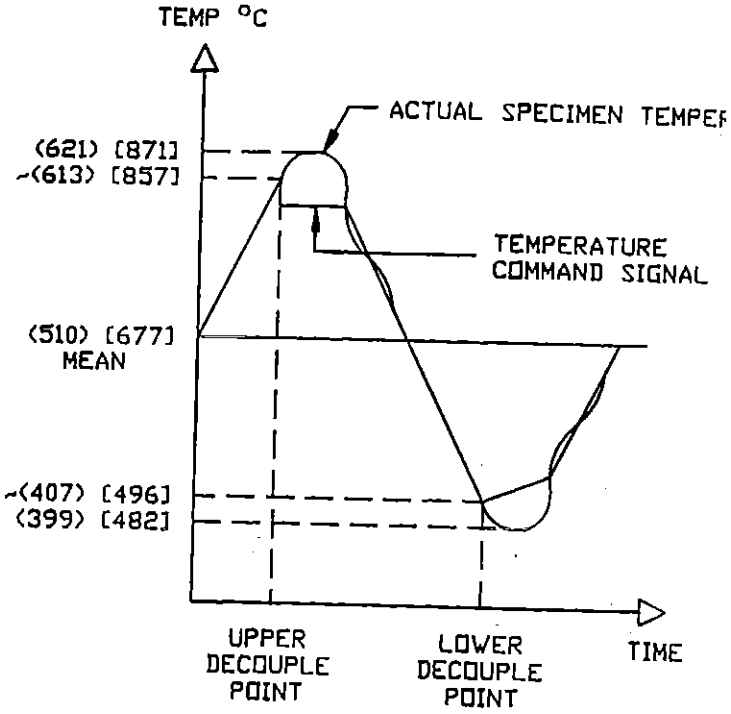

Fig. 4 Temperature command signal and resulting specimen response during TMF experiment without hold-time

Biaxial Experimental Results

Axial-Torsional IP TMF experiments were conducted with a 0.3% to 0.5% mechanical axial strain range superimposed on a 0.3% to 1.45% torsional strain range producing biaxiality ratios, $\lambda = \Delta\gamma/\varepsilon_{mech}$, which varied from 1 to 3.625. The temperature cycle was 399-621 °C (750-1150 °F). Biaxial strain test results for IP TMF are plotted in Figure 5 in terms of von Mises yield criterion along with uniaxial IP and OP TMF and biaxial isothermal fatigue data previously generated.

In general, the IP TMF data generally shows shorter lives than the isothermal data indicating that this type of cycle is more damaging to the life of the 316 SS material. However, most of the damage is attributed to the axial strain components and not the torsional strain component. Typical biaxial IP TMF mid-life hysteresis loops are shown in Figure 6. The total loop is larger than the mechanical loop since the TMF test is IP where thermal and mechanical strains are additive.

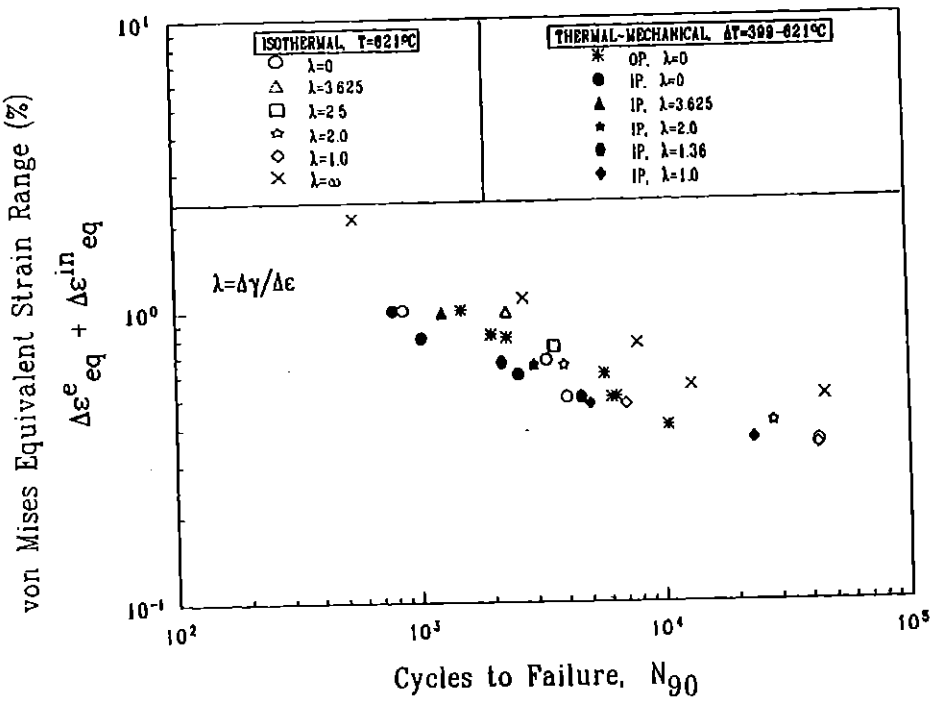

Fig. 5 Correlation of Type 316 SS fatigue data using the von Mises equivalent strain range criterion

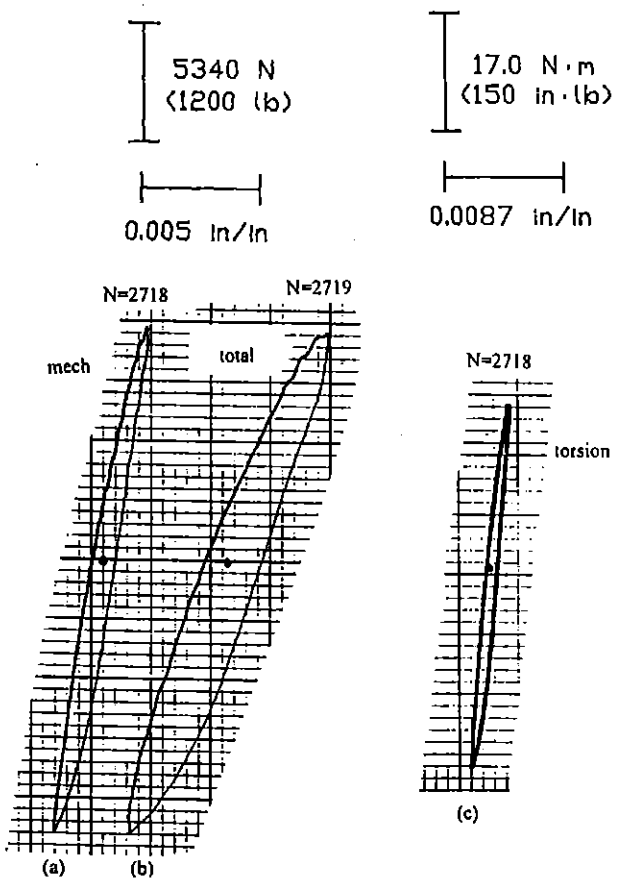

Fig. 6 Typical mid-life hysteresis loops from biaxial IP TMF testing of Type 316 SS. (a) mechanical, (b) total, and (c) torsional. $\Delta\varepsilon_{mech} = 0.4\%$, $\Delta\gamma = 0.4\%$, $\Delta T = 399\text{-}425\ ^{\circ}C$

Development of Biaxial TMF Life Prediction Model

Biaxial fatigue TMF, plotted in Figure 5 on the basis of von Mises criterion, shows considerable scatter in the data which highlights the effect of thermal/mechanical strain cycling. To address this problem, a model has been developed to assess biaxial TMF.

The proposed biaxial TMF model is based on the isothermal biaxial fatigue model developed by Zamrik, Mirdamadi, and Davis [8]. The model had three basic components: triaxiality factor (TF), modified equivalent strain and transition cycle Z-parameter. The triaxiality factor concept, developed by Davis and Connelly [9], is used to show the effect of

state stress on ductility. They proposed that an effective ductility, $\bar{\varepsilon}_f$, under multiaxial loading condition may be obtained by dividing the tensile ductility (tensile elongation), ε_{fo}, by a triaxiality factor:

$$\bar{\varepsilon}_f = \frac{\varepsilon_{fo}}{TF} \tag{1}$$

where:

$$TF = \frac{(\sigma_1 + \sigma_2 + \sigma_3)}{\frac{1}{\sqrt{2}}\left[(\sigma_1 - \sigma_2)^2 + (\sigma_2 - \sigma_1)^2 + (\sigma_3 - \sigma_1)^2\right]^{1/2}} = \frac{J_1}{\sigma_{eq}} \tag{2}$$

The triaxiality factor (TF) is equal to one for uniaxial case, zero for pure torsion case and two for equal biaxial case. Their view was that the effective ductility reduces as TF increases. Manjoine **[10]** has applied the concept of triaxiality factor to explain the effect of stress on ductility at elevated temperatures under monatonic loading. The measure reduction of ductility for a number of materials versus triaxiality factor is shown in Figure 7. Manjoine's experimental results indicated that for a given temperature and strain rate, ductility decreases as triaxiality factor increases.

Zamrik and Mirdamadi **[8]** showed that the triaxiality factor can improve the Mises equivalent strain predictive capability when expressed as:

$$\Delta\varepsilon_{eq}^{t} = \Delta\varepsilon_{eq}^{e} + \Delta\varepsilon_{eq}^{p} \tag{3}$$

$$= B(2N_f)^b + C(2N_f)^c \tag{4}$$

where the constants are replaced by:

$$B = (Z^{1-TF})\frac{\sigma_f'}{E} \tag{5}$$

and

$$C = (\Lambda^{1-TF})\varepsilon_f' \tag{6}$$

Therefore the equivalent strain can now be expressed as:

$$\Delta\varepsilon_{eq}^{t} = Z^{1-TF}\frac{\sigma_f'}{E}(2N_f)^b + \Lambda^{1-TF}\varepsilon_f'(2N_f)^c \tag{7}$$

and the Z-parameter is taken as the ratio of the fatigue transition cycles between the axial and the torsion strain where the elastic strain is equated to the plastic strain and defined as:

$$Z = \frac{3}{2(1+\nu^e)}\frac{\tau_f'/G\varepsilon_f'}{\sigma_f'/E\gamma_f'} \tag{8}$$

Experimental results using the model are shown in Figure 8.

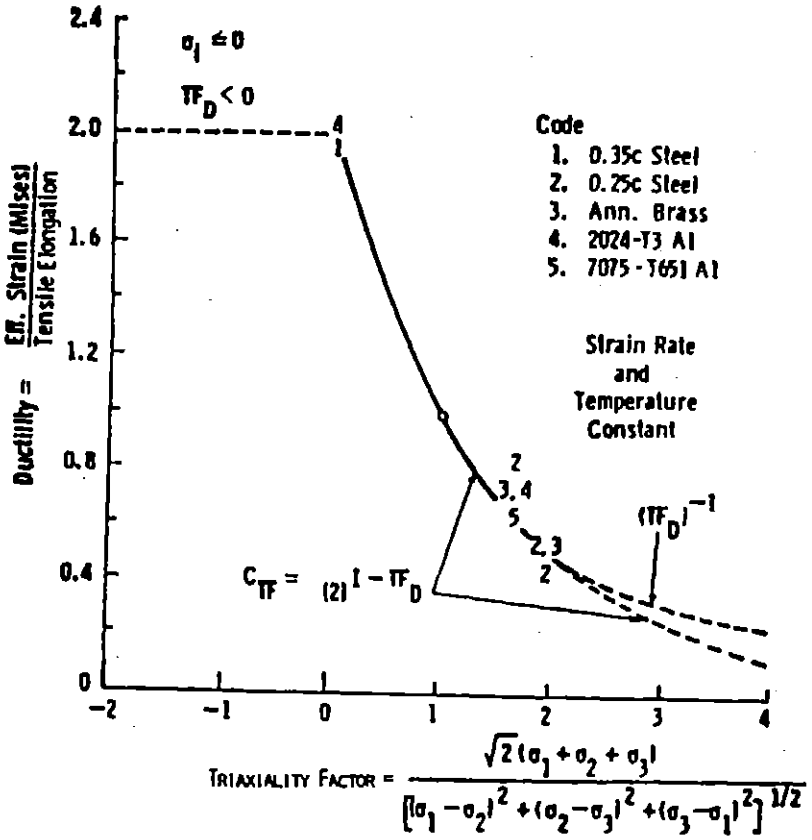

Fig. 7 Effective ductility as a function of stress state as calculated by the triaxiality factor [10]

However, when Equation (7) was applied to IP TMF biaxial fatigue data, considerable scatter was observed and the isothermal approach was still not adequate as shown in Figure 9. One difference between the isothermal data and the TMF data is the cycle frequency. Under TMF, the cycle is much slower than under isothermal cycling and by cycling at a slower rate, creep or environmental damage per cycle can be induced. Therefore, a frequency term, f, has to be included in the inelastic strain term of Equation (7) resulting in:

$$\Delta\varepsilon^{*}_{eq} = (Z^{TF-1})\Delta\varepsilon^{e}_{eq} + (\frac{1}{f})^{m}(\Lambda^{TF-1})\Delta\varepsilon^{p}_{eq} \qquad (9)$$

where $Z = 1.35$, $\Lambda = 2$, $m = 0.10$.

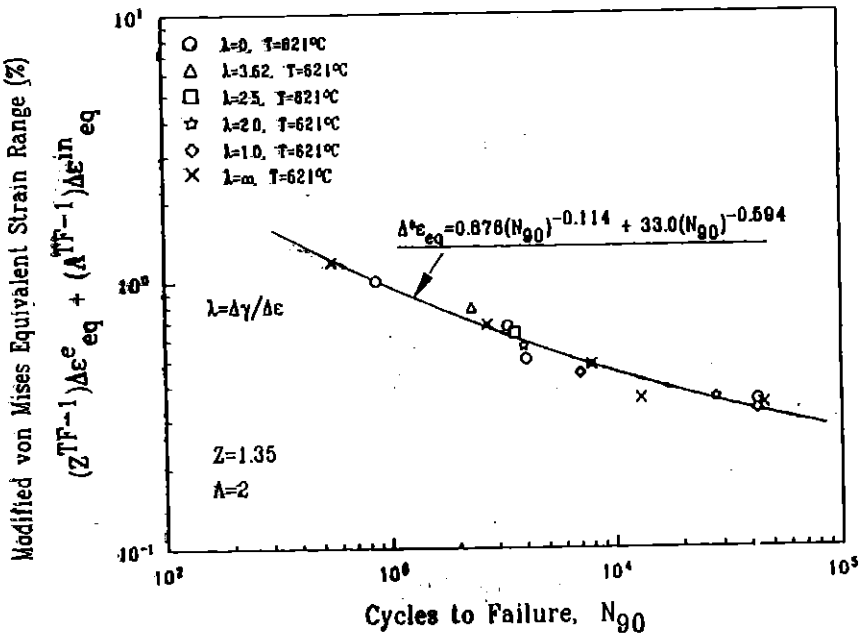

Fig. 8 Analysis of isothermal axial, torsional, and axial-torsional fatigue data on Type 316 SS using "Z-parameter" and triaxiality factor

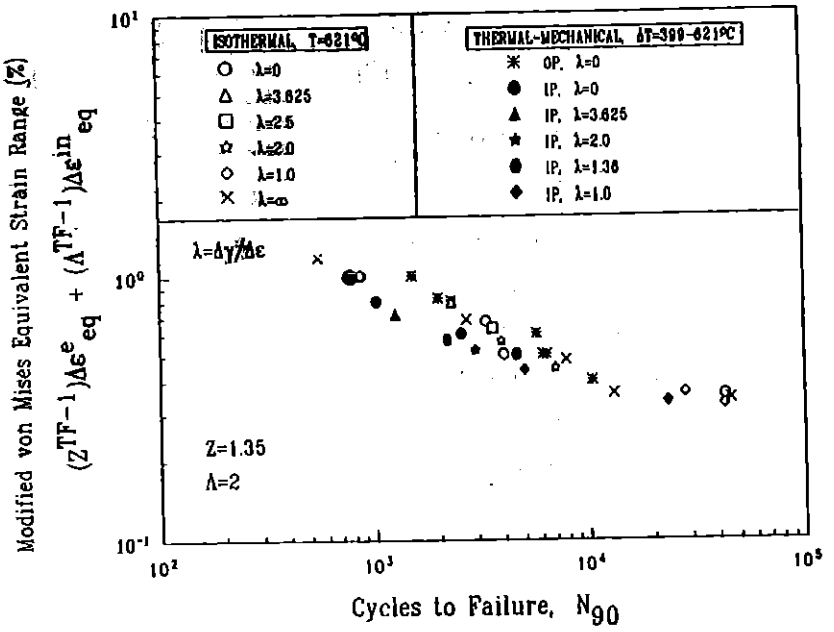

Fig. 9 Analysis of uniaxial and biaxial isothermal and thermal-mechanical fatigue data on Type 316 SS using "Z-parameter" and triaxiality factor

Using Equation (9), isothermal and TMF data is replotted as shown in Figure 10. Two observations can be made from the results: one is that the TMF data has shifted, relative to the isothermal data, towards larger equivalent strain ranges because the IP and OP TMF cycle time is much longer (180 sec) than the isothermal cycle time (6 sec). The second observation is that the OP data lies above the isothermal data while the IP data falls slightly below, suggesting a thermal/mechanical phase effect.

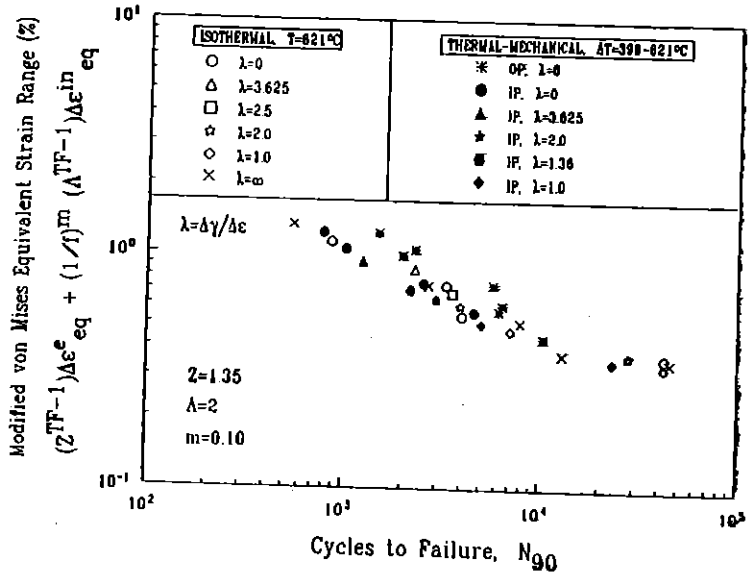

Fig. 10 Analysis of uniaxial and biaxial isothermal and thermal-mechanical fatigue data on Type 316 SS using "Z-parameter", triaxiality factor, and frequency modification.

Neu and Schitoglu [11] proposed specific mathematical relations for thermal/mechanical strain phasing to account for the effect of oxidation and creep damage due to TMF loading. The phasing factor, Φ, is written in the form of two exponential functions in terms of thermal/mechanical strain rates. One function is an oxidation effect under OP TMF and the other for the creep effect encountered in the IP TMF cycle; however, the two phase factors for oxidation and creep may be determined simply by plotting the frequency modified inelastic strain range against life for isothermal IP and OP TMF data sets as shown in Figure 11. The IP and OP phase factors, Φ^{IP} and Φ^{OP}, are then computed from the equivalent strain ratios. For example, at a given life of 2000 cycles, the following ratios were calculated:

$$\Phi^{IP} = \frac{[\Delta\varepsilon^{in}(1/f)^{0.1}]_{iso}}{[\Delta\varepsilon^{in}(1/f)^{0.1}]_{ip}} = \frac{0.47}{0.40} = 1.15 \tag{10}$$

and

$$\Phi^{OP} = \frac{[\Delta\varepsilon^{in}(1/f)^{0.1}]_{iso}}{[\Delta\varepsilon^{in}(1/f)^{0.1}]_{op}} = \frac{0.47}{0.66} = 0.70 \tag{11}$$

Once the phase factors are determined, they are incorporated in the von Mises modified strain range, Equation (9), as:

$$\overset{*}{\Delta\varepsilon}_{eq} = (Z^{TF-1})\,\Delta\varepsilon^{e}_{eq} + \phi\,(1/f)^{m}(\Lambda^{TF-1})\,\Delta\varepsilon^{p}_{eq} \tag{12}$$

where

$$\phi = \begin{Bmatrix} \phi^{OP} \\ 1 \\ \phi^{IP} \end{Bmatrix} : 1 \text{ for isothermal condition} \tag{13}$$

Equation (12) was used to analyze all types 316 SS isothermal and TMF data generated under uniaxial and biaxial loading. The data is plotted in Figure 12. As seen in Figure 12, the proposed model shows excellent ability to predict the fatigue life for the high ductility 316 SS under a variety of uniaxial and biaxial isothermal/TMF conditions.

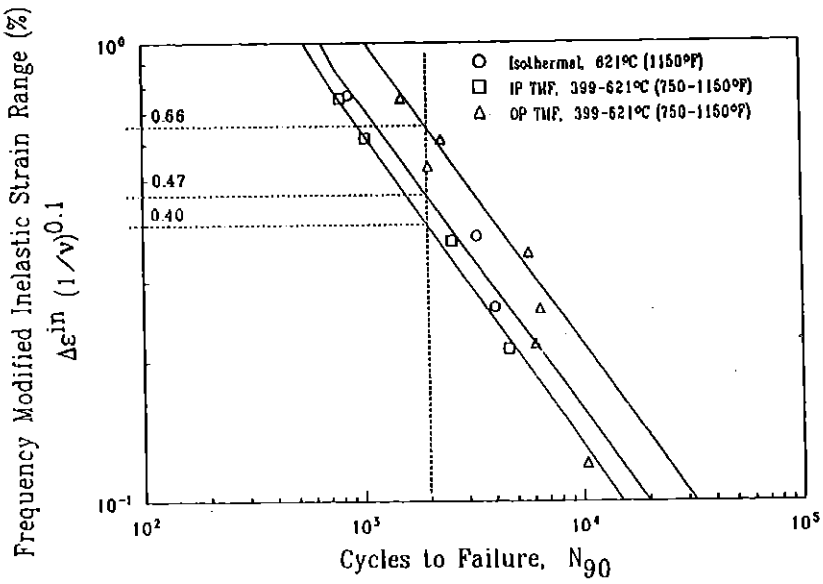

Fig. 11 Identification of IP and OP phase factors for thermal-mechanical strain cycling of Type 316 SS from 399-621 °C

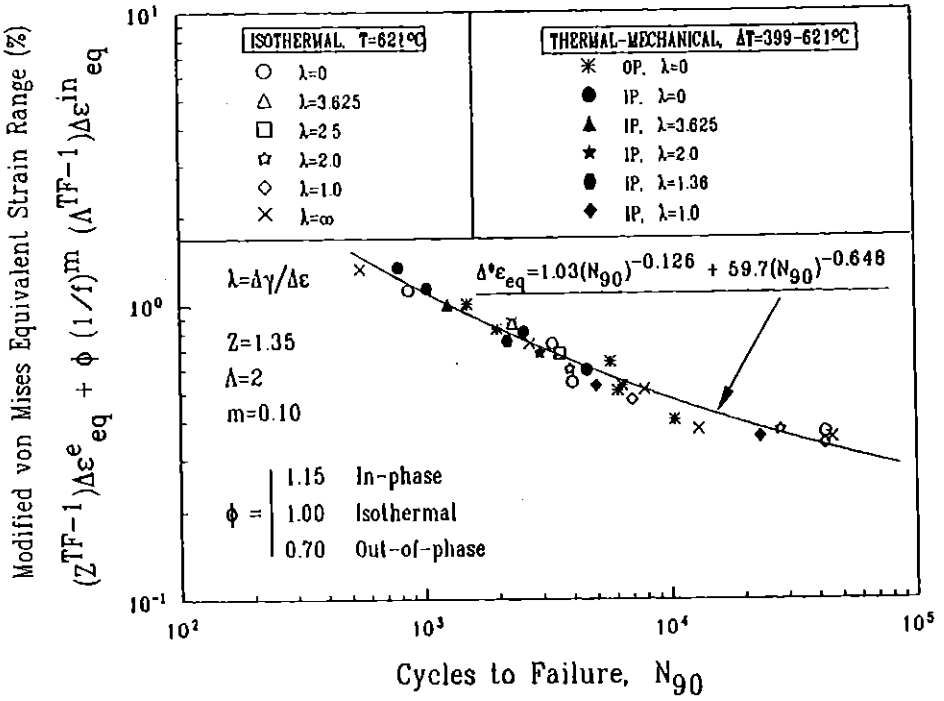

Fig. 12 Analysis of uniaxial and biaxial isothermal and thermal-mechanical fatigue data on Type 316 SS using "Z-parameter", triaxiality factor, frequency modification and phase factor

Summary and Conclusions

The proposed TMF biaxial fatigue model is based on an established isothermal biaxial model to relate uniaxial, torsional and axial-torsional fatigue data. Two parameters, namely frequency and phase factors, are introduced in the model to account for the effect of IP or OP TMF. The effect of frequency on fatigue life at elevated temperature is an important factor since oxidation or creep could become the major damaging mechanism. A previous study by Firth **[12]** on type 316 SS showed that creep damage is the dominant failure mechanism where intergranular cracking occurred during uniaxial IP TMF testing, whereas OP suppressed creep effect and crack growth was transgranular. The microscopic analysis of this study also shows that biaxial IP TMF results primarily in an intergranular failure as shown in Figures 13 and 14. The IP TMF phase factor was 1.15 reflecting the creep damage by increasing the effective inelastic strain range by 15%. On the other hand, the OP TMF phase factor was 0.70 which is an indication that the oxidation was not a factor since

the equivalent strain range was reduced by 30% and the life was increased. The use of Z-parameter, triaxiality factor, frequency and phase factor effect for creep and oxidation, have successfully modeled the biaxial TMF.

Fig. 13 SEM fractograph showng intergranular crack growth in semi-circular intiation region. $\Delta\varepsilon_{mech} = 0.3\%$, $\Delta\gamma = 0.3\%$, IP TMF, $\Delta T = 399\text{-}621°C$, $N_{90} = 23229$.

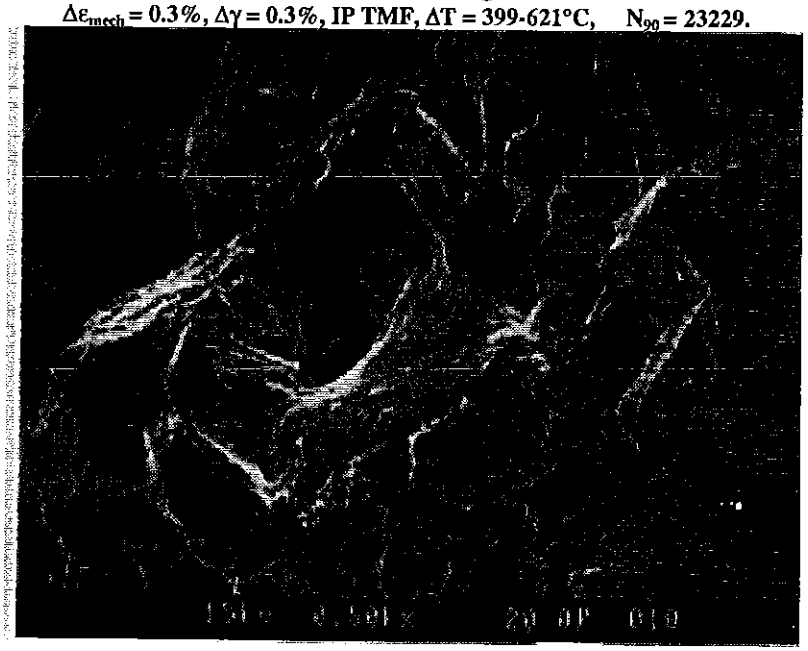

Fig. 14a SEM micrograph showing mixed-mode crack propagation in 316 SS $\Delta\varepsilon_{mech}$ = 0.5%, $\Delta\gamma$ = 0.68%, IP TMF, ΔT = 399-621°C, N_{90} = 2144

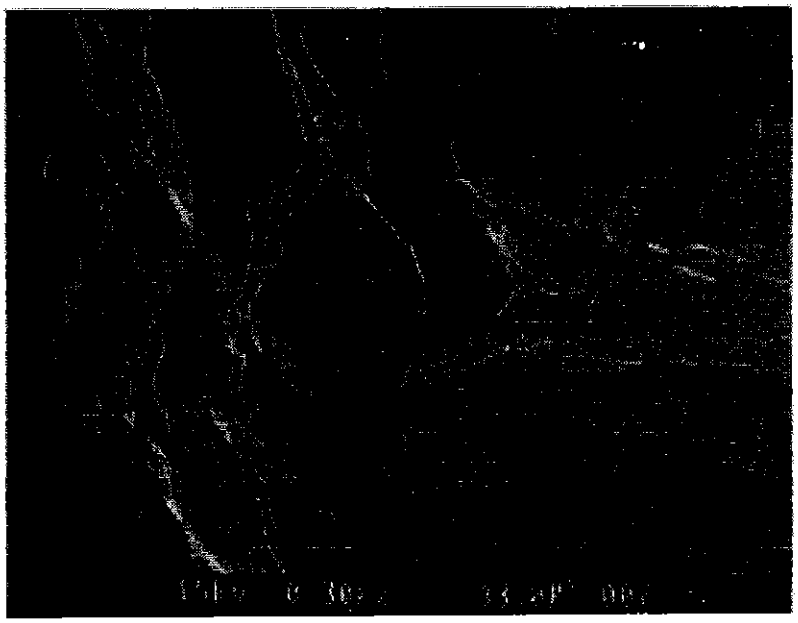

Fig. 14b SEM fractograph showing severe intergranular secondary cracking and severe rubbing on the fracture surface due to a high torsional strain range. $\Delta\varepsilon_{mech}$ = 0.4%, $\Delta\gamma$ = 1.45%, IP TMF, ΔT = 399-621 °C, N_{90} = 1253

References

(1) YAMAUCHI, M., OHTANI, T. and TAKAHASHI, Y., (1996), "Thermal Fatigue Behavior of a SU304 Pipe Under Longitudinal Cyclic Movement of Axial Temperature Distribution," Thermomechanical Fatigue Behavior of Materials: Second Volume, ASTM STP 1263, (M. J. Verrilli and M. G. Castelli, Eds.), American Society For Testing and Materials, Philadelphia, PA.

(2) CASTELLI, M. G., BAKIS, C. E. and ELLIS, J. R., (1992), "Experimental Investigation of Cyclic Thermomechanical Deformation in Torsion," NASA TM-105938.

(3) MEERMAN, J., FRENZ, H., ZEIBS, J., KUHN, H. J. and FOREST, S., (1995), "Thermo-Mechanical Fatigue Behavior of IN738LC and SC16," Thermal Mechanical Fatigue of Aircraft Engine Materials, AGARD-CP-569, 81st Meeting of the AGARD Structures and Materials Panel, Bnaff, Canada, pp.19.1-19.11.

(4) BONACUSE, P. J. and KALLURI, S., (1995), "Axial-Torsional Thermomechanical Fatigue Behavior of Haynes 188 Superalloy," Thermal Mechanical Fatigue of Aircraft Engine Materials, AGARD-CP-569, 81st Meeting of the AGARD Structures and Materials Panel, Bnaff, Canada, pp.15.1-15.10.

(5) BONACUSE, P. J. and KALLURI, S., (1995), "Elevated Temperature and Axial Torsional Fatigue Behavior of Haynes 188," Journal of Engineering Materials and Technology, April 1995, pp.191-199.

(6) SOCIE, D.F., (1987), "Multiaxial Fatigue Damage Models," Journal of Engineering Materials and Technology, vol.109, no.4, pp.293-298.

(7) FATEMI, A., and SOCIE, D. F., (1988), "A Critical Plane Approach to Multiaxial Fatigue Damage Including Out-of-Phase Loading," Fatigue and Fracture of Engineering Materials and Structures, vol.11, no.3, pp.149-165.

(8) ZAMRIK, S. Y., MIRDAMADI, M., and DAVIS, D. C., (1993), "A Proposed Model for Biaxial Fatigue Analysis Using the Triaxiality Factor Concept," Advances in Multiaxial Fatigue, ASTM STP 1191, (McDowell, D. L., and Ellis, R. Eds.), American Society for Testing and Materials, Philadelphia, PA, pp.85-106.

(9) DAVIS, E. A. and CONNELLY, F. M., (1959), "Stress Distribution and Plastic Deformation in Rotating Cyclinders of Strain Hardening Materials," Journal of Applied Mechanics, pp.25-30.

(10) MANJOINE, M. J., (1983), "Damage and Failure at Elevated Temperatures," Journal of Pressure Vessel Technology, vol.105, pp.58-62.

(11) NEU, R. W. and SEHITOGLU, H., (1989), "Thermomechanical Fatigue, Oxidation and Creep: Part II. Life Prediction.," Metallurgical Transactions A, vol.20A, pp.1769-1783.

(12) FIRTH, L. E., (1993), "The Response of 316 Stainless Steel to In-Phase and Out-of-Phase Thermal-Mechanical Fatigue," M. S. Thesis, The Pennsylvania State University.

Acknowledgment This research program has been supported by the National Science Foundation under Grant No. MSS-9215694. The 316 Stainless material was provided by Dr. Robert Swindeman of Oak Ridge National Laboratory. The support received from NSF and Dr. Swindeman is greatly appreciated.